sciendo

DOI 10.2478/ama-2023-0055

acta mechanica et automatica, vol.17 no.3 (2023)
Special Issue "Computational Technologies in Engineering TKI2022"

MATERIAL CHARACTERISTIC OF AN INNOVATIVE STENT FOR THE TREATMENT OF URETHRAL STENOSIS

Jagoda KUROWIAK*, Agnieszka MACKIEWICZ*, Tomasz KLEKIEL*, Romuald BĘDZIŃSKI*

*Faculty of Mechanical Engineering, Department of Biomedical Engineering, University of Zielona Góra, ul. Prof. Z. Szafrana 4, 65-516 Zielona Góra, Poland

j.kurowiak@iimb.uz.zgora.pl, a.mackiewicz@iimb.uz.zgora.pl, t.klekiel@iimb.uz.zgora.pl, r.bedzinski@iimb.uz.zgora.pl

received 24 February 2023, revised 3 May 2023, accepted 3 May 2023

Abstract: The appropriate development and customisation of the stent to the urethral tissues requires the determination of many factors such as strength and degradation. Given the distinctive conditions of urethral tissues, it is important that the design of the stent be properly developed. The selection of a stent material requires knowing its material characteristics and verifying that they are suitable for the future implantation site. In the present study, the development of a polydioxanone (PDO)-based stent was undertaken. The PDO material was fabricated using an additive technique – 3D printing. Then, in vitro tests were performed to determine the degradation time of the material under conditions simulating an aggressive urinary environment. The changes in the parameters of mechanical properties before and after the degradation period were determined, and the changes in the structure of the material before and after degradation were observed. Numerical analysis was performed for the proposed stent design. The results showed that PDO has good mechanical properties, but its degradation time is too short to be used in a urethral stent. Among the innovations of the studies conducted are bending strength tests, which is not a frequently considered aspect so far.

Key words: polydioxanone, urethra, modelling, degradation, mechanical properties

1. INTRODUCTION

The urethra, bladder, kidneys and ureters are the anatomical components of the genitourinary system. This arrangement is a storage as well as a drainage system for urine and other toxins excreted from the body. The urogenital system monitors and controls electrolyte levels; regulates blood volume, pressure and pH; and, in case of men, is also responsible for reproductive functions. The structure of the urethra is formed by two main layers of cells: epithelium and smooth muscle cells. Each of these layers has a specific function. The epithelium of the lower urinary tract primarily constitutes a protective function. It protects the deeper layers of the urethra from the absorption of toxins expelled from the body. Smooth muscle cells, on the other hand, affect the elastic and flexible properties of the urethral tissues. There are also small blood vessels in the urethra, which serve the function of nourishing this tissues [1,2]. The literature indicates problems with the correct use of terminology to describe the anatomy of the urethra, mainly male urethra, which is much more likely to be diseased or damaged. As described by Verla et al. [3], male urethra consists of two main sections (from the bladder to the urethral outlet): posterior urethra and anterior urethra. The posterior urethra is divided into the prostatic and the membranous urethra, while the anterior urethra contains the bulbar and the penile urethra [3].

Currently, urological diseases are a major problem worldwide. Disorders related to urethral functioning not only lead to deterioration of the patients' quality of life and genital incapacity, especially in men, but also generate significant health-care expenses [1,2]. The main and most commonly diagnosed disorder of the urethra is urethral stricture. The clinical symptoms of urethral stricture include urinary problems such as increased micturition with less urine output, lower urinary tract infections, discomfort and decreased quality of life, sepsis, bladder stone formation, kidney failure and, in the most serious cases, death. Urethral stricture occurs as a result of tissues fibrosis, which leads to a reduction in the urethral lumen that impedes the free flow of urine and other metabolic products [4–8]. All kinds of injuries to the epithelial and spongy parts are considered to be the cause of this pathology, which subsequently leads to changes in the cellular matrix of the urethral tissues. The primary activity of the epithelium at the site of injury at the time of malfunction is unable to replace the lost cells, which leads to fibrosis. This phenomenon is followed by the replacement of a healthy connective tissue by densely clustered fibroblasts in the stricture tissues. The ratio of type III collagen to type I collagen present in the tissues also decreases. In addition, dense collagen fibres replace smooth muscle cells, significantly impairing the elasticity of the entire system [1,9,10]. Due to specific physiological conditions of the urethra, which include pressure, flow and the interaction of adjacent structures, the urethral tissues must be properly adapted and sufficiently robust to cope with its normal function. Therefore, mechanical properties of the urethra depend on the structure and thickness of the connective tissue and muscle membrane. These tissues are anisotropic in structure and show a nonlinear stress–strain relationship. This is due to the presence of collagen and elastin fibres as well as biological fluids in the structure of the tissues. It provides the tissues with viscoelastic properties due to the presence of elastin, which is a highly elastic fibre that provides elasticity but low tensile strength, and due to the presence of collagen, which gives stiffness to the tissues [6].

The cause of male urethral stricture can vary. It can be caused by iatrogenic injuries, idiopathic causes, previous infectious disease or external trauma [3,9,11,12]. Mundy and Andrich

DOI 10.2478/ama-2023-0055

[12] indicated that for the strictures occurring in the penile area, iatrogenic trauma (40%) and conditions of inflammation (40%) are the most common causes, while the strictures involving the bladder could arise due to idiopathic (40%) and iatrogenic (35%) causes [12]. The literature is fairly explicit that endoscopic procedures performed to treat benign or neoplastic prostatic growths and bladder pathologies, as well as idiopathic causes of unknown origin and cause, are the most common causes of the urethral strictures.

The treatment and reconstruction of the urethral stricture is still a significant challenge for the urological community. There is still no indication concerning the best method of treating this condition; thus, various methods are used in an attempt to select them appropriately depending on the aetiology of the origin, location and length of the stricture [1]. The oldest method of treating the urethral stenosis is calibration, which aims to dilate the narrowed area using balloons, for example. Unfortunately, this method is only a maintenance and temporary treatment and does not counteract the causes of the tissue fibrosis. Long-term dilatation of the urethral wall can lead to frequent recurrence of the stricture. Another treatment that has been claimed to replace dilation is urethrotomy, which involves incision of the fibrotic tissues. The success of both the dilation and urethrotomy procedures mainly depends on the location and length of the stricture, and their main disadvantage is a high rate of the recurrent strictures. Their effectiveness decreases as the length of the stricture increases. Due to the low success rate of these procedures, their disadvantages and complications, the European Association of Urology (EAU) recommends that these procedures should not be used as a treatment when the length of the segment at which the stenosis occurs is >2 cm [9,13–15].

There is the possibility of using the end-to-end method, which involves cutting out the stenosis and re-anastomosing the tissues. This method can be effective only if the length of the stenosis is <1–2 cm. Another treatment method is plastic reconstruction, or urethroplasty, which involves transplanting the tissue from the oral cavity or bowel mucosa [4,16]. Although urethroplasty shows better long-term success rates than dilation and urethrotomy, unfortunately, problems are still encountered. Bleeding, pain and swelling, contractures and scarring, and disruption of the salivary or gastrointestinal tract can occur at the donor site. On the other hand, complications such as fistula and infections can occur at the transplant site as the transplanted membrane flaps may not function properly in the urine environment [3,4,16,].

Along with the high percentage of surgical failures and problems related to the availability of transplanted tissues, new alternative therapies based on the achievements of material engineering and additive technologies are being sought. The use of available biodegradable materials especially natural polymers (hydrogels, i.e., sodium alginate and chitosan), or synthetic polymers (poly(L-lactide [PLLA], poly-caprolactone [PCL], poly(D,L-lactide-co-glycolide) [PDLLA], poly(lactic-co-glycolic acid) [PLGA], polydioxanone [PDO]) along with 3D printing is a good approach for developing and manufacturing urological stents. Stenting is a good treatment option due to the availability of a wide range of biodegradable polymers. To properly select a material for a urological stent, it is necessary to determine the functional conditions of the stent [6–8,17], which allows determining of the requirements for the design including the selection of the mechanical properties of the material so as to match the mechanical characteristics of the stent appropriate to the deformability of the urethra. The key element that enables the design and fabrication of the optimal biomimetic scaffolds for the urethra is to know the mechanical and material parameters of the urethral tissues [18].

One of the promising materials that can meet the demands of urological stents is PDO. PDO is a fully biodegradable synthetic polymer that has ester and ether groups in its structure. It is believed to have the potential to be a future material for biomedical applications [19–25] due to its good mechanical properties, biocompatibility, low inflammatory response and full metabolisation by the body [26]. Adolffson et al. [25] developed innovative resorbable tourniquets for suspending vascular tissues during surgery. Bands made by the incremental methods with PDO have been tested in vitro in phosphate buffered saline (PBS) solution at 37°C for 10 days, 28 days and 140 days as well as in vivo – they were implanted subcutaneously in horses for the same period. While the fabrication of the bands was not a problem due to the good properties of the material, allowing 3D printing, a significant decrease in the mechanical strength of the in vivo implanted bands was observed as early as 28 days after implantation. Mechanical strength of the bands tested in vitro was significantly higher than that of the bands implanted in vivo. The results suggest that the in vivo environment is much more aggressive towards the tested implant; therefore, the implant degrades much faster in it [25]. Fathi et al., [27] fabricated composite intestinal splicing stents using pure PDO and its PCL composites at different mass ratios by 3D printing. The stents were tested in vitro in simulated intestinal fluid (SIF) and foetal bovine serum (FBS) solutions at 37°C for 3 days, 6 days, 10 days and 20 days, and in vivo by implanting the fabricated stents in the small intestine in pigs. In the in vitro tests, a predictable decrease in the weight of the implant samples associated with decomposition was observed. The maximum weight loss was about 80% after 20 days of the incubation in SIF solution. An in vivo test was conducted on two pigs by splicing the surgically cut intestine at the same locations. One of the pigs showed signs of inflammation and infection due to the rupture of the implant 14 h after implantation, so it was sedated. The other pig did not show similar symptoms, and dissection showed that the implant was accepted and remained tight after a longer period (2 weeks). Microscopic observation using a scanning electron microscope (SEM) showed that the layered design of the implants resulted in better cell adhesion to the implant, which positively affected the healing process [27].

Park et al. [28] investigated the inflammatory response in dogs to the implantation of a urological stent made of PDO wire by manual spinning. Each dog received two implants – a proximal and a distal urethral implant. The dogs were divided into three groups, which were dissected after 4 weeks, 8 weeks and 12 weeks. Implant weight reduction occurred sequentially by 54% after 4 weeks of implantation and by 84% after 8 weeks, and after 12 weeks, the stents were completely dissolved. The study showed a slight inflammatory reaction after the implantation and an increase in the granulation tissue formation with time, but no closure of the urethral lumen [28]. Stehlik et al. [29] implanted dilating tracheal stents made of PDO mono-wire in four patients with tracheal stenosis. All patients showed improvement immediately after the implantation and in the long term. The stents were completely absorbed after 7 months, with endoscopy showing residual traces of the stent implantation in the form of scarring and tissue granulation. The authors noted that due to the decreasing mechanical strength over time, resulting from the degradation of the stent made of PDO compared to, for example, classic stents made of NiTi alloy, recurrence of the tracheal lumen stenosis is possible. Nevertheless, the authors considered this type of im-

plant to be future-proof [29]. Zamiri et al. [30] studied the response to implantation of arterial stents made of various composites including PDO tested in vivo in pigs. The stents were implanted in the carotid arteries and left there for 30 days and 90 days. The animals were investigated for inflammation periodically against the disintegrating stents, and there was little or moderate inflammation in PDO. The authors also noted that the internal diameter of the stent made of PDO after 90 days of implantation in the artery was the smallest of all the tested ones. Considering all the composites and polymers tested, the authors concluded that resorbable materials are suitable for use as the stent materials in less than a year [30].

In the present study, the authors evaluated PDO. In vitro laboratory tests were performed for the requirements of urological stents. Strength requirements were determined by the numerical analysis. To evaluate the mechanical properties of PDO, mechanical tests were performed by static tensile testing and three-point bending. Material degradation tests were performed in an artificial urine environment reflecting the environmental conditions inside the coil including the effect of degradation on the mechanical properties. Fourier-transform infrared spectroscopy (FTIR) analysis and scanning electron microscope (SEM) surface morphology analysis were performed to describe the degradation-induced changes in the material structure.

2. MATERIALS AND METHODS

2.1. Stent deformability analysis

To determine the requirements for the stent, a numerical model, which was developed based the studies on the urethras of New Zealand rabbits, was used [6]. The diameter range of 0–15 mm depending on the pressure inside was assumed as the dimensions of the urethral canal [6]. Since the assumptions made considered that the stenosis covers about 2 cm of the length of the urethra, an implant of the shape, as shown in Fig. 1, was proposed.

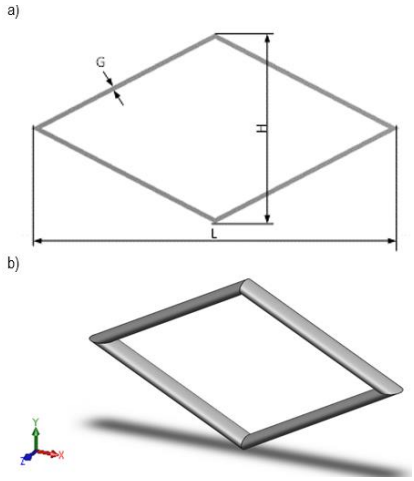

Fig. 1. Stent model: (a) dimensions L = 25 mm, H = 13 mm, G = 2 mm; (b) 3D model

The adopted shape of the stent was subjected to a numerical analysis to determine the values of the relative deformations occurring inside such a structure, resulting in the determination of the limit at which changes caused by the material degradation will cause loss of the stent functionality. The pressure that occurs in the urethral canal of about 15 mBar was taken as the load of the stent [6].

2.2. Materials

In the research, RESOMER Filament X D1.75 Polydioxanone from Evonik (Alabama, USA) was used. The degradation process was carried out in an artificial urine solution, which was prepared according to a commonly used procedure presented in the works mentioned in Refs [7,17,31,32], among others. The solution consisted of urea (Sigma-Aldrich, Poznań, Poland), creatinine (Sigma-Aldrich, Poznań, Poland), sodium chloride NaCl (Sigma-Aldrich, Poznań, Poland), ammonium chloride NH_4Cl (Chempur, Poland), sodium sulphate Na_2SO_4 (Avantor Performance Materials Poland SA, Gliwice, Poland) and disodium phosphate (Avantor Performance Materials Poland SA, Gliwice, Poland). The artificial urine solution was prepared using ultrapure water.

2.3. Sample preparation – 3D printing

To manufacture the PDO specimens, 3D printing realised on a Flashforge Adventurer printer was used. The bending test was performed on perpendicular specimens prepared in accordance with ISO 178:2010 Plastics – Determination of bending properties. The tensile tests were performed on paddle specimens prepared in accordance with ISO 527:1998 Plastics. The determination of mechanical properties in static tension. The tests were carried out on specimens whose dimensions are specified by the mentioned standards.

Samples for bending tests: rectangular specimens were made on a scale of 1:3 (measuring length 26 mm, width 3.33 mm and thickness 1.33 mm).

Samples for tensile tests: paddle samples were made on a scale of 1:4 (measuring length 12.5 mm, width 2.5 mm and thickness 1.0 mm.

The PDO polymer printing parameters were chosen according to the manufacturer's recommendations: nozzle temperature 150°C and table temperature 90°C. Other printing conditions to ensure that PDO specimens are ready for testing are as follows: fill density 100%, printing speed 30 mm/s, traverse speed 30 mm/s and printing accuracy is ± 0.2 mm. In Tab. 1, the nomenclature of the test samples is given.

Tab. 1. Name of the samples tested

Material	Incubation in a degrading environment [days]	Name of the sample
PDO	0	PDO_0d
	1	PDO_1d
	2	PDO_2d
	5	PDO_5d
	7	PDO_7d
	15	PDO_15d
	30	PDO_30d
	45	PDO_45d

PDO, polydioxanone

DOI 10.2478/ama-2023-0055

2.4. In vitro degradation

The degradation studies of PDO were carried out in artificial urine solution, and the mass change evaluation was determined after 0 day, 1 day, 2 days, 5 days, 7 days, 15 days, 30 days and 45 days. For each degradation period, the number of samples was *n* = 5. The obtained results were averaged. For the purpose of replicating the conditions as closely as possible, the degradation tests were carried out using an Avantgarde Line BD115 incubator (Binder GmbH, Tuttlingen, Germany) providing a constant temperature of 37°C. The samples were stored separately in sterile and tightly sealed polypropylene (PP) containers filled with 15 ml of the urine solution. The urine solution was replaced every 7 days. Change in the material weight due to degradation was calculated from relation (1):

$$\text{Weight change } [\%] = \left(\frac{M_{\text{wet}} - M_{\text{dry}}}{M_{\text{wet}}}\right) * 100\% \quad (1)$$

where M_{wet} is the initial mass of the sample and M_{dry} is the mass of the sample dried after immersion in the artificial urine solution.

2.5. Tensile strength

The tensile tests were performed on paddle specimens (Fig. 2) prepared in accordance with PN-EN ISO 527:1998 Plastics. The determination of mechanical properties in static tension. The tests were performed for PDO specimens after the process of manufacturing by 3D printing, until their destruction. Based on the tests, Young's modulus (E), tensile strength (Rm) and yield strength (Re) were determined. The number of test specimens was *n* = 5. The testing speed was 15 mm/min. The research conditions were as follows: temperature 23°C and air humidity 40%. During the degradation, the pH of the artificial urine solution was monitored using an Elmetron CPI-505 pH meter (Elmetron, Zabrze, Poland).

Fig. 2. PDO samples manufactured by 3D printing – for tensile strength testing. PDO, polydioxanone

2.6. Bending test

The strength tests determining the bending properties for the PDO material were performed on a Zwick Roell EPZ 005 testing machine (Zwick Roell, Ulm, Germany). The bending test was carried out in accordance with the requirements described in ISO 178:2010.

The perpendicular specimens (Fig. 3.) were made on a scale of 1:3: measurement length L = 26 mm, width b = 3.33 mm and thickness h = 1.33 mm (dimensional accuracy due to the manufacturing technology was ± 0.2 mm).

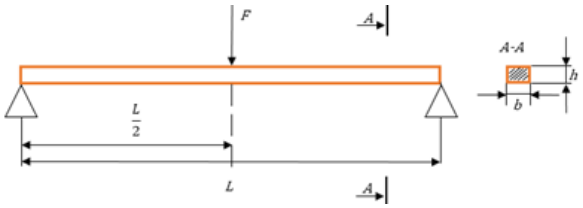

Fig. 3. Three-point bending test

The tests were conducted for the material before and after the specified degradation time (0 day, 1 day, 2 days, 5 days, 7 days, 15 days, 30 days and 45 days). After each degradation time, Young's modulus of the five specimens was determined with three replicates of each specimen (*n* = 15). The test speed was 0.1 mm/s. The assumed deflection for each repetition was 1 mm. This is the parameter that allows performing of a non-destructive bending test. The tests made it possible to determine such parameters as the longitudinal elastic modulus – Young's modulus (E), bending strength (σg) and strain (ε). The material, after being drawn from the urine, was placed in the designed holder, and the bending process was started. The test conditions were as follows: temperature 23°C and humidity 40%.

The value of Young's modulus was determined according to the following steps:

I. Measurement of the parameters of the test sample: width (b), thickness (h) and measurement length (L).
II. The deflection (s) for the test specimen was determined, assuming s = 1 mm.
III. The plotting of force–displacement curves for a given deflection, reading the force (F) for a deflection of 1 mm.
IV. The calculation of the value of Young's modulus from relation (2):

$$E = \left(\frac{3FL^3}{8bh^3s}\right) \quad (2)$$

where F is the maximum force for deflection [N], L is the measurement length [mm], b is the specimen width [mm], h is the specimen height [mm] and s is the deflection.

Presentation of the obtained results of the calculated Young's modulus on a box plot.

2.7. FTIR-ATR analysis – Fourier-transform infrared spectrometry

The purpose of this research was to evaluate the chemical structure of the PDO material before and after incubation in an artificial urine solution. It was important to see if there are chemical changes in the material during the degradation process that could negatively affect the stent–tissue interactions. Infrared spectroscopy studies were performed using a Thermo Scientific Nicolet iS50 FTIR spectrometer (Thermo Fisher Scientific, Massachusetts, USA). FTIR spectra were measured in the range from 500 cm^{-1} to 4,000 cm^{-1}, using an ATR detector at a resolution of 16 scans per spectrum and an optical resolution of 4 cm^{-1}. The ATR crystal was thoroughly cleaned with an alcohol-soaked tissue paper before and after each measurement. Before a new measurement, the background spectrum was measured and collected. The analysis was carried out at ambient temperature. Before the analysis, the samples were air-dried for 24 h to get rid of water molecules that could distort the spectrum. The measurements were made in triplicate for each degradation time, which were then averaged.

2.8. SEM microscopy analysis

The surface of the PDO polymer was examined using a scanning electron microscope SEM (JEOL, JSM-7600F, Tokyo, Japan). The purpose of this study was to characterise changes in the morphology of the material occurring as a result of its degradation. Before the material was placed in the chamber and imaged, the samples were coated with a 9-nm-thick chromium conductive layer (QUORUM Q150TS). The structure of the material was observed at 1,500× magnification using a voltage of 15 kV.

3. RESULTS AND DISCUSSION

Numerical analysis for the assumed stent shape made it possible to determine how changes in the material properties affect the deformability of the adopted stent model. Fig. 4a shows the deformation of the stent at 15 mbar for the material in its original form, that is, before the degradation process. Reinforcement of the material due to degradation caused the strain in the radial direction to the coil channel to decrease by about 30% under the same loading conditions (Fig. 4b.).

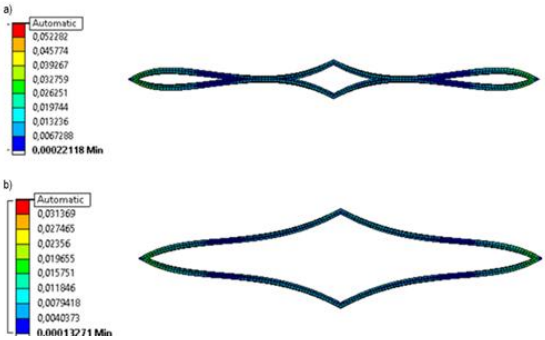

Fig. 4. Stent deformability under a circumferential pressure of 15 mBar for (a) material PDO before degradation test, (b) material PDO after 45 days degradation test. PDO, polydioxanonez

The bending test was carried out on a degradable material and was a non-destructive test. It showed that during the degradation process of the stent made of PDO, its increased stiffness caused a decrease in the kinetics of the coil wall, which promotes both better micturition and generate problems related to the tissue fibrosis.

3.1. In vitro degradation

Degradation of the PDO material was evaluated by observing the change in its weight mass calculated from relation (1). Fig. 5 shows the results obtained. After 45 days of urine interaction simulating the conditions conducive to the degradation of this material, it was observed that for the first period of degradation (0–5 days), there was no significant weight change in the material (<1%). After 7 days, a slight decrease in the weight of the samples of about 2.5% was observed, while on the 45th day, the weight of the samples decreased by an average of about 15% from the initial weight. The measurement uncertainty was determined to be ±0.0021 g. This value is not statistically significant. The pH value of the urine solution was monitored during the degradation studies. The average pH value was 6.55, which is within the range of normal urine pH, that is, 4.5–8.0

It is widely accepted that the degradation time of PDO is <6 months [33–35]. From the degradation tests obtained in this study, a slight change in weight was observed, but the changes that occurred resulted in a decrease in the material strength.

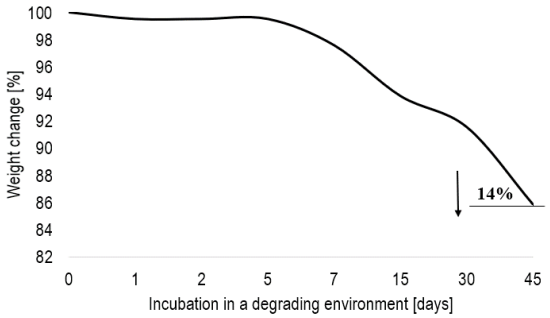

Fig. 4. Weight change of PDO material degraded in artificial urine solution. PDO, polydioxanone

3.2. Tensile strength

Strength tests for the static tensile test (Figs. 6 and 7) showed that Young's modulus value was 450.68 MPa (418.75 MPa; 506.80 MPa), the tensile strength was 43.07 MPa (40.48 MPa; 45.11 MPa) and the yield strength was 9.79 MPa (9.04 MPa; 11.06 MPa). Bezrouk et al. [24] in their study on commercially available stents made of a PDO monofilament showed that their average Young's modulus value was 958 MPa [24]. Similar results were obtained by Loskot et al. [20], where average Young's modulus value for the specimens was 965 MPa.

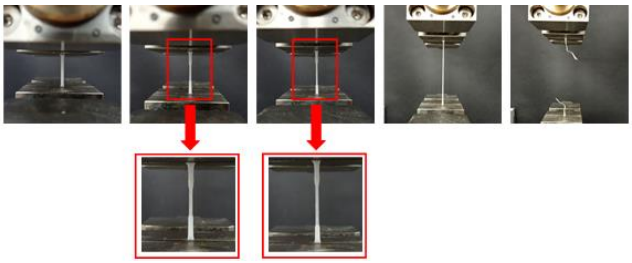

Fig. 5. Static tensile test of PDO – example photo of a sample. PDO, polydioxanone

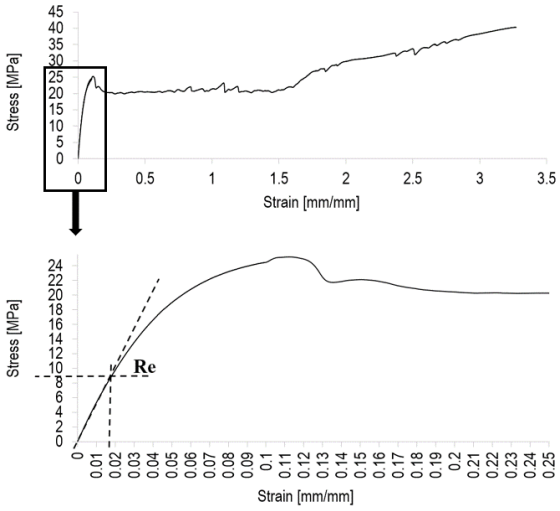

Fig. 6. Stress–strain curves for PDO static tensile testing. PDO, polydioxanone

DOI 10.2478/ama-2023-0055

3.3. Bending test

To evaluate the functionality of the stent, it was necessary to determine the mechanical properties of the material in question. In case of urological stents, it is desirable that the material used and the design of the stent allow high deformability. This high deformability should allow for large changes in the cross-sectional area of the urethra, which are naturally induced by the pressure changes and the activity of muscles acting in the urethra. This behaviour of the stent should be the stent's response to the urethral wall endeavour to close the channel. At the same time, this mechanical mismatch and low biocompatibility between the stent and the tissues can lead to restenosis or hyperplasia of the tissue structure.

The bending test performed (Fig. 8a,b.) for the printing PDO materials allowed the determination of Young's modulus (E) (Fig. 9). From the data obtained, it can be seen that the longer the degradation time in a fluid simulating urine, the higher the stiffness of the material. There was an increase in the maximum bending stress with a simultaneous increase in the value of the longitudinal modulus (E).

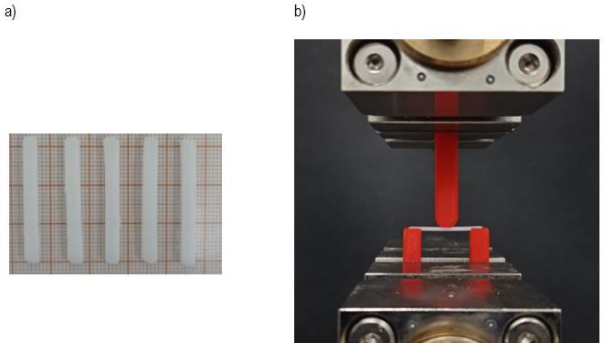

Fig. 7. PDO specimens produced by 3D printing technology (a), flexural strength test rig with a mounted specimen (b).
PDO, polydioxanone

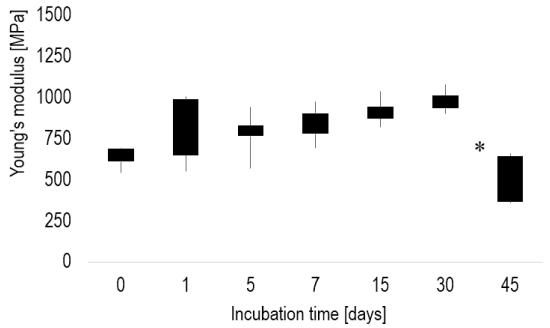

Fig. 8. Young's modulus of PDO material as a function of degradation time in urine. PDO, polydioxanone

Based on the results, it was also analysed how the average maximum force and Young's modulus (Tab. 2) changed during the deflection. The longer the incubation time in the urine environment, the higher the maximum force. This observation applies to studies involving up to 30 days of incubation. After the 45th day of the degradation, there was a sharp decrease in the maximum force along with a loss of mechanical properties of the PDO material. The material became brittle and much less strong, leading to failure at only 13.8% of the initial force. Lower values for Young's modulus obtained in this study are most likely due to the different methods adopted for manufacturing of the samples and their different geometries. The higher the material Young's modulus, the higher its stiffness, and therefore, the less it deforms. Given the results analysed in relation to the urethral conditions, it is important to obtain the highest possible deformability, rather than stiffness, of the material.

Tab. 2. Summary of the average values of the action of maximum forces and the average values obtained for Young's modulus

	0 days deflection 1 mm	1 days deflection 1 mm	2 days deflection 1 mm	5 days deflection 1 mm	7 days deflection 1 mm	15 days deflection 1 mm	30 days deflection 1 mm	45 days* deflection 0.2 mm
Mean maximum strength [N]	0.94	1.14	1.15	1.16	1.22	1.35	1.46	**0.18**
Mean value of Young's Modulus [MPa=N/mm^2]	631.63	772.06	774.16	779.58	826.56	908.03	980.56	488.91

* The loss of mechanical properties of the PDO material.

Conderman et al. [36] presented a mechanical analysis of a cartilage graft that was reinforced with a plate made of PDO. Young's modulus value in their study for PDO was 692 ± 37.4 MPa. At the same time, it should be noted that in case of Conderman's study, the bending test for the PDO material was performed for the material using a different manufacturing procedure with no degradation process [36].

3.4. FTIR-ATR analysis – Fourier spectrometry in infrared

The characteristics of the FTIR spectra for the PDO material are presented in Fig. 10.

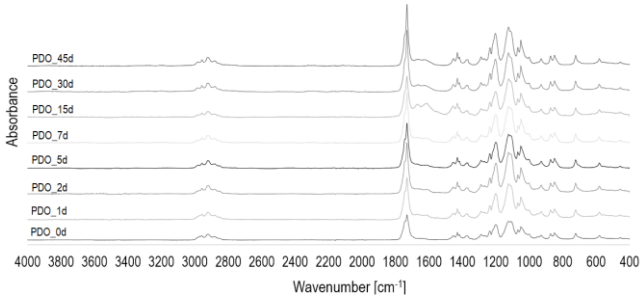

Fig. 9. FTIR spectra of the PDO material before and after a specified incubation time in artificial urine solution.
FTIR, Fourier transform infrared; PDO, polydioxanone

The observed peaks correspond to and characterise the occurrence of individual functional groups. Peaks in the range from 3,000 cm^{-1} to 2,800 cm^{-1} are characteristic of symmetric and asymmetric vibrations of the C-H group of the aliphatic chain. A strong single peak corresponding to C=O stretching vibrations located in the ester carbonyl group for each of the degradation periods after averaging was recorded at 1,731.95 cm^{-1}. The peaks in the range from 1,200 cm^{-1} to 1,000 cm^{-1} are characteristic of asymmetric C-O stretching vibrations, while the peak near 850 cm^{-1} indicates the presence of symmetric C-O stretching vibrations. The peak observed near 1,431 cm^{-1} indicates the presence of bending vibrations of the C-H group. Deeper analysis of the different parts of the FTIR spectra did not reveal any deviations in the bands; therefore, it can be concluded that no new functional groups were formed during the degradation. This is

important from the point of view of the safety of using the PDO material in living organisms, especially if it stays in the body for >30 days. Li et al. [19] and Loskot et al. [37] obtained similar results, which may confirm that the degradation of the PDO material in fluids simulating the given environment is safe for the organism.

3.5. SEM microscopy analysis

Fig. 11 presents the obtained surface morphologies of the PDO material before and after temporary degradation at 1,500× magnification. The material before degradation (Fig. 11a) shows a smooth and homogeneous surface. The material shows deposited urine solution particles after 1 day, 2 days, 5 days, 7 days and 15 days of degradation, respectively (Fig. 11b–f.). However, after 30 days and 45 days of incubation in urine solution, cracks were observed on the material surface (Fig. 11g,h.). The number of cracks present after 30 days of degradation is quite large, and after 45 days, the number of cracks and deformation of the polymer fibres is even larger and more pronounced.

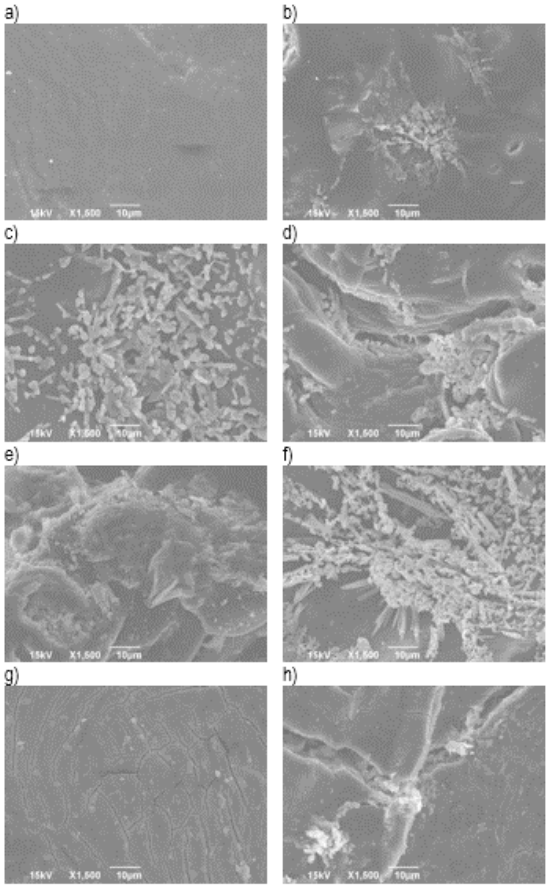

Fig. 10. Morphology of the PDO material surface before and after degradation: (a) before degradation, (b) after 1 day of incubation, (c) after 2 days of incubation, (d) after 5 days of incubation, (e) after 7 days of incubation, (f) after 15 days of incubation, (g) after 30 days of incubation, (h) after 45 days of incubation. PDO, polydioxanone

The characteristic arrangement of the cracks on the polymer surface indicates that the material is losing its elasticity and resilience, becoming a more brittle and vulnerable material. It can be assumed that the action of stimuli and external forces on such a degraded material can cause serious damage and even prevent it from performing its function of decongesting the channel of the narrowed urethra. Microscopic observations of the material structure confirm the mechanical strength results that the material after 45 days of incubation in the urine environment is fully degraded, becomes brittle and loses its mechanical properties.

4. CONCLUSION

The analysis of the PDO material shows good mechanical properties, while the degradation time for the fabricated material is too short to be used as a urethral stent. Given the minimum of 60–90 days needed for the full regeneration of the urethral tissues, a change in the manufacturing method or an additive to the material produced by 3D printing should be considered to extend the degradation time. The success of the research is the testing of flexural strength, which is not a frequently considered aspect so far. With specific conditions in the urethra during the urine flow, it is important that the material used for the stent has high deformability. This is necessary due to the action of varying external forces on the urethra both from outside in the form of the muscle action and inside in the form of the urine pressure. During micturition, neighbouring muscles act on the urethra, which induces high stresses in the tissues. The research and results will serve as a prelude to further analysis for similar applications of PDO material in tissue engineering.

REFERENCES

1. Tan Q, Le H, Tang C, Zhang M, Yang W, Hong Y, Wang X. Tailor-made natural and synthetic grafts for precise urethral reconstruction. J. Nanobiotechnology. 2022;20(392):1–23. https://doi.org/10.1186/s12951-022-01599-z
2. Xu K, Han Y, Huang Y, Wei P, Yin J, Jiang J. The application of 3D bioprinting in urological diseases. Mater. Today Bio. 2022;16 (100388):1–17. doi: 10.1016/j.mtbio.2022.100388
3. Verla W, Oosterlinck W, Spinoit AF, Waterloos M. A Comprehensive Review Emphasizing Anatomy, Etiology, Diagnosis, and Treatment of Male Urethral Stricture Disease. BioMed Res. Int. 2019;2019: 9046430:1–20. doi: 10.1155/2019/9046430
4. Lazzeri M, Sansalone S, Guazzoni G, Barbagli G. Incidence, Causes, and Complications of Urethral Stricture Disease. Eur. Urol. Suppl. 2016;15(1):2–6. 10.1016/j.eursup.2015.10.002
5. Yao HJ, Wei ZW, Wan X, Tao YC, Zhang DC, Wang Z, Xie MK. Three new experimental models of anterior urethral stricture in rabbits. Transl. Androl. Urol. 2022;11(6):761–772. doi: 10.21037/tau-22-104
6. Klekiel T, Mackiewicz A, Kaczmarek-Pawelska A, Skonieczna J, Kurowiak J, Piasecki T, Noszczyk-Nowak A, Będziński R. Novel design of sodium alginate based absorbable stent for the use in urethral stricture disease. J. Mater. Res. Technol. 2020;9(4):9004–9015. https://doi.org/10.1016/j.jmrt.2020.06.047
7. Kurowiak J, Mackiewicz A, Klekiel T, Będziński R. Evaluation of Selected Properties of Sodium Alginate-Based Hydrogel Material-Mechanical Strength, μDIC Analysis and Degradation. Materials. 2022;15(3):1–15. https://doi.org/10.3390/ma15031225
8. Mackiewicz A, Klekiel T, Kurowiak J, Piasecki T, Będziński R. Determination of Stent Load Conditions in New Zealand White Rabbit Urethra. J. Funct. Biomater. 2020;11(4):1–9. https://doi.org/10.3390/jfb11040070
9. Farzamfar S, Elia E, Chabaud S, Naji M, Bolduc S. Prospects and Challenges of Electrospun Cell and Drug Delivery Vehicles to Correct Urethral Stricture. Int. J. Mol. Sci. 2022;23(18):1–37. https://doi.org/10.3390/ijms231810519

DOI 10.2478/ama-2023-0055

10. Basikn LS, Constantinescu SC, Howard PS, Mcaninch JW, Ewalt DH, Duckett JW, Snyder HM, Macarak EJ. Biomechanical characterization and quantitation of the collagenous components of urethral stricture tissue. J. Urol. 1993;150:642–647. 10.1016/s0022-5347(17)35572-6
11. Goel A, Goel A, Jain A, Singh BP. Management of panurethral strictures. Indian J. Urol. 2011;27(3):378–384. 10.4103/0970-1591.85443
12. Mundy AR, Andrich DE. Urethral strictures. BJU International. 2010;107(1):6–26. doi: 10.1111/j.1464-410X.2010.09800.x.
13. Engel O, Soave A, Rink M, Fisch M. Reconstructive Management with Urethroplasty. European Association of Urology. 2016;15(1):13–16. 10.1016/j.eursup.2015.10.004
14. Pudełko P. Rekonstrukcja cewki moczowej - uretroplastyka/Reconstruction of the urethroplasty. Przegląd Urologiczny. 2016;96.
15. Pastorek D, Culenova M, Csobonyeiova M, Skuciova V, Danisovic L, Ziaran S. Tissue Engineering of the Urethra: From Bench to Bedside. Biomedicines. 2021:9(12):1–12. 10.3390/biomedicines9121917
16. Cheng L, Li S, Wan Z, Huang B, Lin J. A brief review on anterior urethral strictures, Asian J Uro. 2018;5(2):88–93. 10.1016/j.ajur.2017.12.005
17. Kurowiak J, Kaczmarek-Pawelska A, Mackiewicz A, Będziński R. Analysis of the Degradation Process of Alginate-Based Hydrogels in Artificial Urine for Use as a Bioresorbable Material in the Treatment of Urethral Injuries. Processes. 2020;8(3):1–11. https://doi.org/10.3390/pr8030304
18. Cunnane EM, Davis N, Cunnane CV, Lorentz KL, Ryan AJ, Hess J, Weinbaum JS, Walsh MT, O'Brien FJ, Vorp DA. Mechanical, compositional and morphological characterisation of the human male urethra for the development of a biomimetic tissue engineered urethral scaffold. Biomaterials. 2021;269(120651):1–31. 10.1016/j.biomaterials.2021.120651
19. Li G, Li Y, Lan P, Li J, Zhao Z, He X, Zhang J, Hu H. Biodegradable weft-knitted intestinal stents: Fabrication and physical changes investigation in vitro degradation. J. Biomed. Mater. Res. Part A. 2014;102(4):982–990. https://doi.org/10.1002/jbm.a.34759
20. Loskot J, Jezbera D, Zmrhalová ZO, Nalezinková M, Alferi D, Lelkes A, Voda P, Andrýs R, Myslivcová-Fučiková A, Hosszŭ T, Bezrouk A. A Complex In Vitro Degradation Study on Polydioxanone Biliary Stents during a Clinically Relevant Period with the Focus on Raman Spectroscopy Validation. Polymers. 2022;14(5):1–19. https://doi.org/10.3390/polym14050938
21. Zilberman M, Eberhart RC. Drug-Eluting Bioresorbable Stents for Various Applications. Annu. Rev. Biomed. Eng. 2006;8:153–180. https://doi.org/10.1146/annurev.bioeng.8.013106.151418
22. Zhang W, Kanwal F, Fayyaz M, Rehman UR, Wan X. Efficacy of Biodegradable Polydioxanone and Polylactic Acid Braided Biodegradable Biliary Stents for the Management of Benign Biliary Strictures. Turk J Gastroenterol. 2021;32(8):651–660. 10.5152/tjg.2021.201174
23. Kwon C, Son JS, Kim KS, Moon JP, Park S, Jeon J, Kim G, Choi SH, Ko KH, Jeong S, Lee DH. Mechanical properties and degradation process of biliary self-expandable biodegradable stents. Dig Endosc. 2021;33(7):1158–1169. doi: 10.1111/den.13916
24. Bezrouk A, Hosszu T, Hromadko L, Olmrova-Zmrhalova Z, Kopecek M, Smutny M, Krulichova IS, Macak JM, Kremlacek J. Mechanical properties of a biodegradable self-expandable polydioxanone monofilament stent: In vitro force relaxation and its clinical relevance. PLOS ONE. 2020;15(7):1–16. https://doi.org/10.1371/journal.pone.0235842
25. Adolfsson KH, Sjöberg I, Hőglund OV, Wattle O, Hakkarainen M. In Vivo Versus In Vitro Degradation of a 3D Printed Resorbable Device for Ligation of Vascular Tissue in Horses. Macromol. Biosci. 2021;21(10):1–12. https://doi.org/10.1002/mabi.202100164
26. Saska S, Pilatti L, Santos de Sousa Silva E, Nagasawa MA, Câmara D, Lizier N, Inger E, Dyszkiewicz-Konwińska M, Kempisty B, Tunchel S, Blay A, Shibil JA. Polydioxanone-Based Membranes for Bone Regeneration. Polymers. 2021;13(11):1–16. https://doi.org/10.3390/polym13111685
27. Fathi P, Capron G, Tripathi I, Misra S, Ostadhossein F, Selmic L, Rowitz B, Pan D. Computed Tomography-Guided Additive Manufacturing of Personalized Absorbable Gastrointestinal Stents for Intestinal Fistulae and Perforations. Biomaterials. 2020,228(119542):1–36. doi: 10.1016/j.biomaterials.2019.119542
28. Park JH, Song HY, Shin JH, Kim JH, Jun EJ, Cho YC, Kim SH, Park J. Polydioxanone Biodegradable Stent Placement in a Canine Urethral Model: Analysis of Inflammatory Reaction and Biodegradation. J Vasc Interv Radiol. 2014;25(8):1257–1264. 10.1016/j.jvir.2014.03.023
29. Stehlik L, Hytych V, Letackova J, Kubena P, Vasakova M. Biodegradable polydioxanone stents in the treatment of adult patients with tracheal narrowing. BMC Pulm. Med. 2015;15(164):1–8 10.1186/s12890-015-0160-6
30. Zamiri P, Kuang Y, Sharma U, Ng TF, Busold RH, Rago AP, Core LA, Palasis M. The biocompatibility of rapidly degrading polymeric stents in porcine carotid arteries. Biomaterials. 2010;31(31):7847–7855. 10.1016/j.biomaterials.2010.06.057
31. Kurowiak J, Kaczmarek-Pawelska A, Mackiewicz A, Baldy-Chudzik K, Mazurek-Popczyk J, Zaręba Ł, Klekiel T, Będziński R. Changes in the Mechanical Properties of Alginate-Gelatin Hydrogels with the Addition of Pygeum africanum with Potential Application in Urology. Int. J. Mol. Sci. 2022;23(18):1–16. https://doi.org/10.3390/ijms231810324
32. Chutipongtanate S, Thongboonnkerd V. Systematic comparisons of artificial urine formulas for in vitro cellular study, Anal. Biochem. 2010;402(1):110–112. 10.1016/j.ab.2010.03.031
33. Gil-Castell O, Badia JD, Bou J, Ribes-Greus A. Performance of Polyester-Based Electrospun Scaffolds under In Vitro Hydrolytic Conditions: From Short-Term to Long-Term Applications. Nanomaterials. 2019;9(5):1–19. https://doi.org/10.3390/nano9050786
34. Zhao F, Sun J, Xue W, Wang F, King MW, Yu C, Jiao Y, Sun K, Wang L. Development of a polycaprolactone/poly(p-dioxanone) bioresorbable stent with mechanically self-reinforced structure for congenital heart disease treatment, Bioact. Mater. 2021;6(9):2969–2982. https://doi.org/10.1016/j.bioactmat.2021.02.017
35. Tian Y, Zhang J, Cheng J, Wu G, Zhang Y, Ni Z, Zhao G. A poly(L-lactic acid) monofilament with high mechanical properties for application in biodegradable biliary stents. J. Appl. Polym. Sci. 2020;138(2):1–8. https://doi.org/10.1002/app.49656
36. Conderman C, Kinzinger M, Manuel C, Protsenko D, Wong BJF. Mechanical analysis of cartilage graft reinforced with PDS plate. Laryngoscope. 2013;123(2):339–343. doi: 10.1002/lary.23571
37. Loskot J, Jezbera D, Bezrouk A, Doležal R, Andrýs R, Francová V, Miškář D, Myslivcová-Fučiková A. Raman Spectroscopy as a Novel Method for the Characterization of Polydioxanone Medical Stents Biodegradation. Materials. 2021;14(18):1–16. https://doi.org/10.3390/ma1

Acknowledgments: "The work has been accomplished under the research project No. DEC-2016/21/B/ST8/01972, funded by National Science Center, Poland".

Jagoda Kurowiak: https://orcid.org/0000-0003-2692-5311

Agnieszka Mackiewicz: https://orcid.org/0000-0002-3956-8483

Tomasz Klekiel: https://orcid.org/0000-0002-2699-3528

Romuald Będziński: https://orcid.org/0000-0003-3611-2584